Received: 3 October 2023 | Revised: 11 January 2024 | Accepted: 7 February 2024

DOI: 10.1002/alz.13776

Alzheimer's & Dementia®
THE JOURNAL OF THE ALZHEIMER'S ASSOCIATION

RESEARCH ARTICLE

Structural white matter properties and cognitive resilience to tau pathology

Ting Qiu[1] | **Zhen-Qi Liu**[2] | **François Rheault**[3] | **Jon Haitz Legarreta**[4] | **Alex Valcourt Caron**[5] | **Frédéric St-Onge**[1] | **Cherie Strikwerda-Brown**[1,6] | **Amelie Metz**[1] | **Mahsa Dadar**[1,7] | **Jean-Paul Soucy**[2] | **Alexa Pichet Binette**[8] | **R. Nathan Spreng**[1,2,7] | **Maxime Descoteaux**[5] | **Sylvia Villeneuve**[1,7] | **for the PREVENT-AD Research Group**

[1]Douglas Mental Health University Institute, Montreal, Canada

[2]Montreal Neurological Institute, Department of Neurology and Neurosurgery, McGill University, Montreal, Canada

[3]Medical Imaging and NeuroInformatics Lab, Université de Sherbrooke, Sherbrooke, Canada

[4]Department of Radiology, Brigham and Women's Hospital, Mass General Brigham/Harvard Medical School, Boston, Massachusetts, USA

[5]Sherbrooke Connectivity Imaging Laboratory, Université de Sherbrooke, Sherbrooke, Canada

[6]School of Psychological Science, The University of Western Australia, Perth, Australia

[7]Department of Psychiatry, McGill University, Montreal, Canada

[8]Clinical Memory Research Unit, Faculty of Medicine, Lund University, Lund, Sweden

Correspondence
Sylvia Villeneuve, Douglas Mental Health University Institute, Perry Pavilion Room E3417.1 6875 Boulevard LaSalle, Montréal, QC Canada H4H 1R3.
Email: Sylvia.villeneuve@mcgill.ca

Funding information
Chinese Scholarship Council, Grant/Award Number: 201906070287; Canadian Institutes of Health Research foundation; Alzheimer's Society Canada and Brain Canada Research

Abstract

INTRODUCTION: We assessed whether macro- and/or micro-structural white matter properties are associated with cognitive resilience to Alzheimer's disease pathology years prior to clinical onset.

METHODS: We examined whether global efficiency, an indicator of communication efficiency in brain networks, and diffusion measurements within the limbic network and default mode network moderate the association between amyloid-β/tau pathology and cognitive decline. We also investigated whether demographic and health/risk factors are associated with white matter properties.

RESULTS: Higher global efficiency of the limbic network, as well as free-water corrected diffusion measures within the tracts of both networks, attenuated the impact of tau pathology on memory decline. Education, age, sex, white matter hyperintensities, and vascular risk factors were associated with white matter properties of both networks.

DISCUSSION: White matter can influence cognitive resilience against tau pathology, and promoting education and vascular health may enhance optimal white matter properties.

Highlights:

- Aβ and tau were associated with longitudinal memory change over ~7.5 years.
- White matter properties attenuated the impact of tau pathology on memory change.
- Health/risk factors were associated with white matter properties.

KEYWORDS
amyloid-β, cognitive resilience, default mode network, limbic network, tau, white matter

1 | BACKGROUND

Alzheimer's disease (AD) is a progressive disorder characterized by the accumulation of amyloid-β (Aβ) plaques and tau tangles in the brain, which starts years before clinical symptom onset.[1] The accumulation of Aβ and tau arises in a selective spatiotemporal manner, propagating across intrinsic brain networks.[2,3] The limbic network comprises the anterior temporal, portions of the insular and the ventromedial prefrontal cortices, and the default mode network (DMN) comprises the medial prefrontal cortex, posterior cingulate, angular gyri, and medial and lateral temporal lobes.[4] These networks are vulnerable to Aβ and tau pathology[3,5] and are involved in cognitive processes like memory, attention, and emotion processing.[4,6] While higher levels of Aβ and tau pathology are typically associated with cognitive decline, there are interindividual variabilities in the cognitive vulnerability to AD pathology, such that some older adults maintain normal cognition despite the presence of significant pathology.[7,8] This phenomenon is known as "cognitive resilience". There is substantial interest in identifying factors that enhance cognitive resilience given that delaying the onset of symptoms by just 1 year would reduce the prevalence of AD dementia by more than 10%.[9,10]

Various lifestyle and health factors, such as higher education, increased physical activity, and lower vascular risk factors, have been consistently linked to cognitive resilience in AD.[11,12] Those modifiable risk factors have been suggested to enhance tolerance to AD pathology through functional and structural coping mechanisms.[13] Advanced imaging techniques, including positron emission tomography (PET) and magnetic resonance imaging (MRI), now allow us to test these hypotheses in vivo.[13] Functional MRI studies have shown that among individuals with AD, higher levels of functional connectivity in the left frontal cortex can attenuate the effect of tau pathology on cognition.[14] Increased functional network segregation was also found to predict lower impact of tau pathology on cognitive performance.[10] In parallel, a recent study showed that higher levels of white matter connectivity moderated the negative association between brain atrophy, white matter hyperintensities (WMHs), and cognitive function.[15]

Our goal was to examine the possible moderation and mediation effect of macro-structural and/or micro-structural white matter properties on the association between AD pathology (Aβ and tau assessed with PET) and longitudinal memory changes in cognitively unimpaired older adults at risk of AD dementia. We focus on two main AD-related networks: the limbic network and the DMN. From a macro-structural perspective, we tested whether global efficiency of the limbic network and the DMN contributes to cognitive resilience to AD pathology. Global efficiency is a measure of information transfer efficiency between brain regions.[16] It has been repeatedly associated with cognitive performance in older participants[17–19] and could play a key role in cognitive resilience.[20] As for the association with micro-structural white matter properties, we tested if free-water (FW) corrected fractional anisotropy (FA_T, where T stands for tissue), FW-corrected mean diffusivity (MD_T), FW-corrected radial diffusivity (RD_T), FW-corrected axial diffusivity (AD_T), and FW index within the tracts of both networks contributed to cognitive resilience. When compared to the traditional diffusion tensor image (DTI) measures, FW-corrected DTI measures provide more robust representation of white matter properties by minimizing the influence of extracellular water.[21] In this context, FA_T assesses the directional consistency of water diffusion, indicative of tissue micro-structural integrity, while MD_T reflects the overall diffusional movement, sensitive to cellular and membrane changes.[21,22] RD_T captures diffusion across fibers, which is linked to myelin sheath status and axonal alterations. AD_T measures diffusion along nerve fibers, and it is associated with axonal health.[21,22] These micro-structural white matter properties are essential for signal transmission and network integration and their integrity has been associated with cognitive performances.[23,24] Last, we assessed which health/lifestyle factors influence macro- and micro-structural white matter properties, to inform about potential pathways by which cognitive resilience could be improved.

2 | METHODS

2.1 | Participants

We included 194 participants at risk of sporadic AD from the Presymptomatic Evaluation of Experimental or Novel Treatments for AD (PREVENT-AD) study[25,26] who (1) had both Aβ- and tau-PET, (2) had structural and diffusion MRI imaging, (3) were cognitively unimpaired at the time of the PET and MRI imaging scans, and (4) had a minimum of two cognitive assessments. The inclusion and exclusion criteria can be found in Figure S1. After imaging processing and quality control (QC), we excluded three participants due to inadequate PET-MRI image co-registration. Furthermore, one participant was removed for poor registration between T1-weighted (T1w) MRI and diffusion-weighted

MRI (dMRI), and another was excluded for motion artifacts during dMRI scanning (QC details provided in the Tables S1–S2 and Figures S2–S3). As a result, the final sample included 189 participants.

PREVENT-AD is a monocentric longitudinal study that enrolled 387 cognitively unimpaired older adults with a familial history of AD dementia.[25,26] The enrollment criteria included: (1) having a parent or multiple siblings (two or more) diagnosed with AD-like dementia; (2) having intact cognition at enrollment; (3) being age 60 years or older, or between 55 and 59 if <15 years from their affected family member's age at symptom onset; (4) having no major neurological or psychiatric diseases.[25,26] All participants exhibited unimpaired cognitive and functional scores on the Montreal Cognitive Assessment (MoCA) and the Clinical Dementia Rating (CDR) at enrollment and exhibited unimpaired neuropsychological function on the Repeatable Battery for the Assessment of Neuropsychological Status (RBANS) at their baseline visit. Fifteen individuals with ambiguous MoCA, CDR, or RBANS scores at enrollment or baseline visits were considered unimpaired after more extensive neuropsychological testing and were included in the PREVENT-AD cohort.

All participants gave written informed consent in accordance with medical ethics approval of the research project before enrollment.

RESEARCH IN CONTEXT

1. **Systematic review**: We reviewed the literature on Alzheimer's disease, cognitive resilience, risk factors, and brain mechanism using PubMed. Numerous studies have shown that various factors such as education, midlife activities, lifestyle, genetics, and medical history are associated with lower cognitive impairment and dementia risk. However, the underlying brain mechanism behind this protective effect remains unknown.
2. **Interpretation**: We showed that macro- and microstructural white matter properties of structural networks moderate the association between tau pathology and longitudinal memory change in preclinical AD. Education, age, sex, white matter hyperintensities, and a history of hypertension were associated with unfavorable white matter properties. These findings suggest that macro- and micro-structural white matter properties influence cognitive resilience to tau pathology.
3. **Future directions**: Future work is necessary to identify the impact of health/risk factors on longitudinal white matter changes and how these changes affect longitudinal cognition.

2.2 | Neuropsychological testing

Participants underwent annual cognitive evaluation with the RBANS, which comprises 12 subtests that encompass five cognitive domains (mean cognitive follow-up time of 7.43 years ± 1.82, range 1.99–10.24 years). Given that memory is usually the first cognitive domain affected in AD,[27] analyses have been restricted to Immediate Memory (list learning and story memory subtests) and Delayed Memory (list recall, list recognition, story memory, and figure recall subtests) composite scores.

2.3 | Image acquisition

For all participants, MRI data were acquired on a 3 T Siemens Prisma scanner. T1w MRI scans were acquired using a three-dimensional (3D) magnetization prepared rapid gradient echo (MPRAGE) sequence with repetition time (TR) = 2300 ms, echo time (TE) = 2.96 ms, inversion time = 900 ms, flip angle = 9°, matrix size = 256 × 256 × 192, voxel size = 1 × 1 × 1 mm, generalized auto-calibrating partially parallel acquisition (GRAPPA) acceleration factor = 2, and duration of 5 min 30 s. T2-weighted (T2w) MRI scans were performed using a 3D T2w SPACE sequence with TR = 2500 ms, TE = 198 ms, turbo factor = 143, matrix size = 320 × 320 × 320, voxel size = 0.64 × 0.64 × 0.64 mm, GRAPPA acceleration factor = 4, and duration of 7 min 35 s. The dMRI scans were acquired using a pulse gradient spin echo (PGSE) EPI sequence with TR = 3000 ms, TE = 66 ms, flip angle = 90°, matrix size = 110 × 110 × 81, voxel size = 2 × 2 × 2 mm, b = [0, 300, 1000, 2000] s/mm^2 with [9, 7, 29, 64] directions, GRAPPA acceleration factor = 2, multiband/SMS factor = 3, and duration of 5 min 49 s. To correct for EPI-induced distortions, a $b = 0$ image with reversed phase-encoding was acquired immediately after the dMRI acquisition. T1w and dMRI scans were the closest available to the date of PET scan (average time between PET and MRI: 1.41 ± 0.99 years).

PET scans were performed on a brain-dedicated Siemens/CTI high-resolution research tomograph using [^{18}F]NAV4694 for measuring Aβ burden and flortaucipir [^{18}F]AV-1451 (FTP) for assessing tau deposition. Aβ-PET scans were obtained 40–70 minutes after injection (220 ± 22 MBq), while tau scans were acquired 80–100 minutes post-injection (370 ± 37 MBq). The acquisition process involved capturing 5-minute frames along with an attenuation scan. Subsequently, after application of standard corrections, the acquired images were reconstructed using a 3D ordinary Poisson ordered subset expectation maximum (OP-OSEM) algorithm with 10 iterations and 16 subsets.

2.4 | PET processing

PET images were processed with a standard pipeline from the Villeneuve lab (see https://github.com/villeneuvelab/vlpp for more details). Aβ- and tau-PET images were realigned, averaged, and co-registered to their corresponding T1w MRI scans, which had been processed and segmented according to the Desikan-Killiany atlas[28] with FreeSurfer 5.3 to define regions of interest in each participant's native space. The registered PET images were then masked to remove cerebrospinal fluid (CSF) signal and smoothed using a Gaussian kernel

of 6 mm^3. Standardized uptake value ratios (SUVRs) were calculated using the cerebellum cortex as the reference region for Aβ-PET images[29] and the inferior cerebellar gray matter for tau-PET images.[30] A global Aβ burden was generated by averaging the SUVR values across the bilateral medial and lateral frontal, parietal, and temporal regions.[31] The assessment of tau pathology was done using a temporal meta-region of interest (meta-ROI), which involved averaging the SUVR of the bilateral entorhinal, amygdala, parahippocampal, fusiform, inferior temporal, and middle temporal regions.[32]

2.5 | Diffusion MRI processing

We used TractoFlow Atlas-Based Segmentation (TractoFlow-ABS) pipeline, an extension of TractoFlow, to process dMRI data (https://github.com/scilus/tractoflow-ABS).[33,34] The functions in TractoFlow/TractoFlow-ABS are based on several neuroimaging software packages, namely, the Diffusion Imaging for Python library (DIPY), MRtrix3, the FMRIB software library (FSL), and ANTs.[33] The pipelines used Nextflow and Singularity to ensure efficient and reproducible processing results for diffusion image analyses.[33] Preprocessing steps include denoising, correction for field inhomogeneity, geometric distortions, eddy-current effects, along with brain extraction, normalization, and upsampling to 1 mm.[33] Specifically, we used the $b = 0$, 300, and 1000 shells to perform tensor fitting to generate maps for the DTI measures, such as FA, MD, RD, and AD. Along with the typical DTI modeling, we used the $b = 0$, 1000, and 2000 shells to perform Constrained Spherical Deconvolution (CSD)[35,36] to compute fiber orientation distribution function (fODF) maps.[37,38] Then the advanced fODF measures like apparent fiber density (AFD, a measure in each fixel, that is, fiber population within voxels proportional to the volume of axons aligned on a specific direction),[37,39] were also generated. Unlike the standard version of TractoFlow, TractoFlow-ABS uses FreeSurfer output files to create tracking and seeding masks robust to WMHs. This approach is favorable for aging brains since these WMHs usually create holes in the white matter mask produced by classical techniques, such as ANTs and FSL.[34,40] It allows for the reconstruction of a more accurate white matter mask, enabling tractography through white matter lesions if coherent local orientations are present.[34] The tracking mask was generated by combining the white matter mask and nuclei masks, and the seeding mask was the white matter and gray matter interface. Last, we performed local probabilistic tracking algorithm using the fODF image for directions and seeding 20 seeds per voxel in the seeding mask, to generate the whole brain tractogram for each participant.[33,41] The tractograms had a mean of 4.32 million streamlines with a standard deviation of 0.56 million streamlines.

2.6 | White matter hyperintensities quantification

WMHs measurement was generated using T1w and T2w MRI scans and a previously validated automated technique[42,43] (see Supplementary methods for details).

2.7 | Network construction

We applied the Connectoflow pipeline (https://github.com/scilus/connectoflow) to construct a whole brain structural network for each participant (step 1 in Figure 1). The pipeline requires the T1w and dMRI images, an atlas for parcellation, tractogram, and fODF image as inputs. The Connectoflow pipeline features a tractogram filtering method: COMMIT2, which is an advanced iteration of Convex Optimization Modeling for Microstructure Informed Tractography (COMMIT).[44,45] This method aims to remove invalid streamlines and assigns a quantitative weight to each streamline, quantifying their actual contributions toward the diffusion signal.[45] We used the AFD metric, a reliable axonal density estimation[37] to weigh the COMMIT2-derived tractograms, providing a region-to-region structural connectivity estimation. This method makes structural connectivity between brain regions more biologically relevant and provides a more faithful representation of the underlying white matter pathway.[46] Given our focus on the limbic network and DMN, we used the Schaefer parcellation with 400 parcels across seven networks as our template to define network nodes.[47] The Schaefer atlas was derived from a sample of 1489 individuals,[47] and while it was originally derived from resting-state fMRI data, it is now widely used across imaging modalities, facilitating comparison with existing literature on brain properties.[10,48] We used FreeSurfer 5.3 output files and the approach detailed on the website to project the Schaefer parcellation into individual space (https://github.com/ThomasYeoLab/CBIG/tree/master/stable_projects/brain_parcellation/Schaefer2018_LocalGlobal).

2.8 | Macro- and micro-structural measurements

After network construction, we extracted the limbic network and DMN from the whole brain network (step 2 in Figure 1). Then we calculated the global efficiency of each network as our macro-structural measurements (step 3–4 in Figure 1). Global efficiency measures the efficiency of transferring distant information in a specific network. It is defined as the average inverse shortest path length, that is, $E = \frac{\sum_{j\in N; j\neq i} d_{ij}^{-1}}{n(n-1)}$, where d_{ij} is the length of the shortest path between node i and j, N is the set of all nodes in the network, and n is the number of nodes.[49]

At the micro-structural level, we filtered tracts connected to regions within the limbic network and DMN, and extracted the weighted average of diffusion measurements within the tracts for both networks (step 3–4 in Figure 1) by using scilpy (version 1.1.0) scripts (https://github.com/scilus/scilpy). Our measures of interest were the FW-corrected DTI measures, namely FA_T, MD_T, RD_T, AD_T, and FW index generated from freely available Freewater_flow pipeline (https://github.com/scilus/freewater_flow).[21,50-52] In brief, the FW elimination model was utilized to estimate and remove the contamination of water from the estimated diffusion tensor of the tissue.[21] This was achieved by fitting a regularized bi-tensor model within each voxel, which models the isotropic diffusion of the FW fraction and tissue compartment.[21] The FW fraction was determined using an isotropic mean diffusivity of 3.0×10^{-3} mm^2/s, a parallel diffusivity of 1.5×10^{-3} mm^2/s and

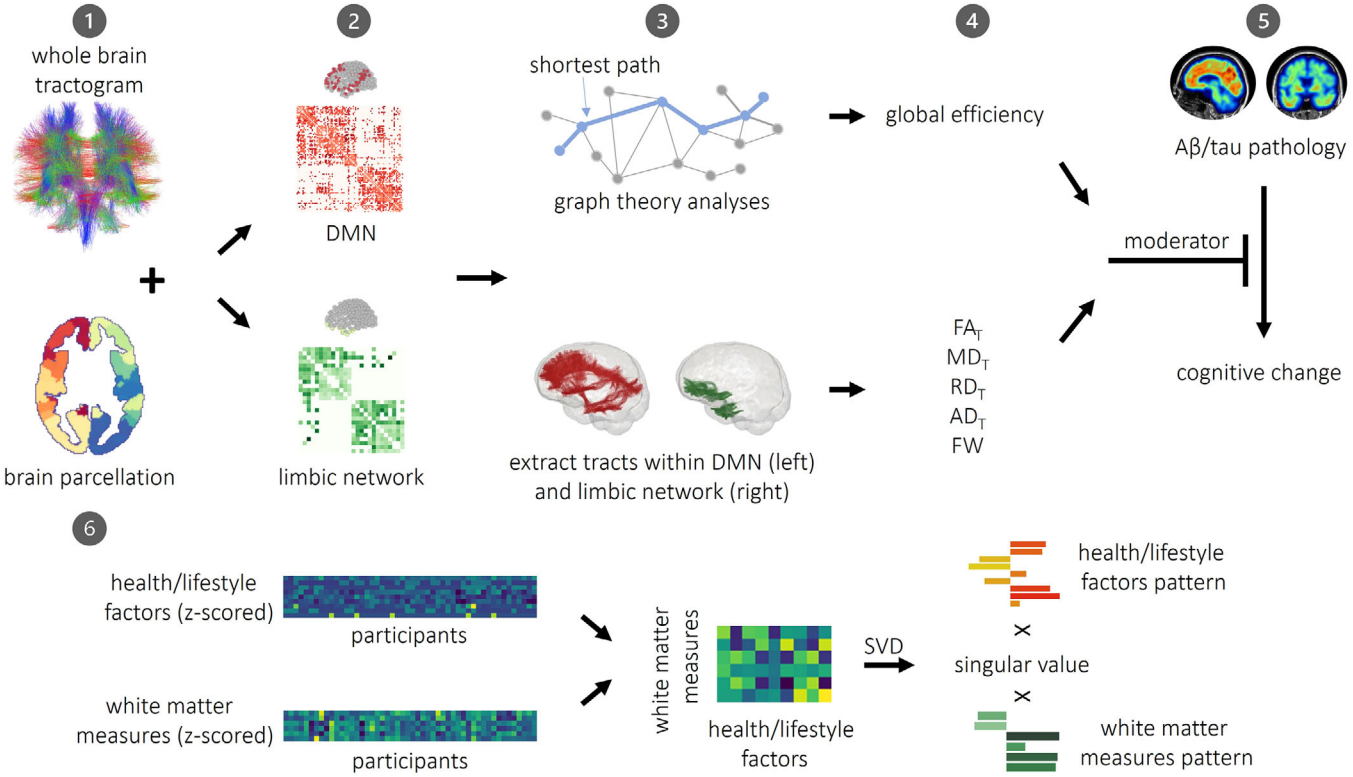

FIGURE 1 Methodology overview. The whole-brain network was constructed using whole-brain tractogram and brain parcellation (step 1); the limbic network and the DMN were extracted from the whole-brain networks (step 2), and graph theory analysis was applied to calculate the global efficiency of the two networks, respectively (step 3–4); tracts that connected regions of the limbic network and the DMN were extracted and weighted average diffusion metrics within the tracts of both networks were calculated (step 3–4); multiple linear regression models were performed to examine the potential moderation effect of global efficiency/diffusion metrics of the limbic network and the DMN on pathological-cognitive associations (step 5). Multivariate PLS analyses were conducted to examine the relationship between the macro-/micro-structural white matter measurements of the structural networks, and health/lifestyle factors (step 6). AD_T, free-water corrected axial diffusivity; DMN, default mode network; FA_T, free-water corrected fractional anisotropy; FW, free-water index; MD_T, free-water corrected mean diffusivity; RD_T, free-water corrected radial diffusivity; PLS, partial least square; SVD, singular value decomposition

regularization parameters of $\lambda_1 = 0$; $\lambda_2, \lambda_3 = 0.25$.[40] As for the tissue compartment, it models the restricted or hindered diffusion of water molecules near the cell membranes in the brain using a diffusion tensor.[40]

2.9 | Statistical analyses

We employed linear mixed-effects models to compute the annual change in both immediate and delayed memory performance for each participant (See Supplementary methods). We then tested whether higher levels of Aβ/tau pathology are associated with faster immediate and delayed memory decline, using linear regression models controlling for age and sex. We also tested the associations between AD pathology and white matter measurements controlling for age and sex. We next investigated the potential moderating role of white matter characteristics (used as continuous variables) within the limbic network and DMN on the relationship between Aβ/tau pathology and memory decline by adding white matter characteristics (e.g., global efficiency) as interactive terms in our linear regression models (step 5 in Figure 1). To mitigate the multicollinearity issues, we mean-centered both the independent variable and the moderator when performing moderation models. Age, sex, and gray matter volume (divided by total intracranial volume) of the regions for the network tested were included as covariates. Given the strong association between education and cognitive resilience,[53,54] education was not included as a covariate in the main models. We also conducted supplementary analyses that incorporated apolipoprotein E (APOE) ε4 status as a covariate in our models. Given that the inclusion of this covariate did not alter our main findings, these additional results with the education adjusted results are presented in the supplementary section for reference (see Supplementary results). We further conducted mediation (rather than moderation) analyses using mediation models with 1000 bootstrapped iterations to analyze the indirect effects of macro-/micro-structural white matter properties considering that AD pathology could influence white matter properties and the latter could then influence cognition. We consider two-sided p-values ≤0.05 after false discovery rate (FDR) correction for multiple comparisons as significant. See Tables S3–S6 for the p-values after FDR correction. As a last step, we performed multivariate partial least square (PLS) analyses to examine the relationship between the macro-/micro-structural white matter measurements of the structural networks, and demographics (i.e., age, sex,

TABLE 1 Sample demographics and variables of interest

Measures	Sample size ($N = 189$)
Age, years	67.83 (±4.88; 58.59–83.22)
Sex, F (%)	136 (71.96)
APOE ε4 carriers, *n* (%)	79 (41.80)
Education, years	15.50 (±3.11; 7–24)
spEYO, years	−4.42 (±7.49; −21.64–26.49)
MMSE score[a]	28.92 (±1.19; 24–30)
Total WMH load (cm^3)[b]	5.25 (±4.78; 1.14–36.10)
LDL value (mmol/L)[c]	2.95 (±0.86; 0.64–5.15)
HDL value (mmol/L)[c]	1.52 (±0.39; 0.78–3.04)
Hypertension, *n* (%)	46 (24.34)
Diabetes, *n* (%)	6 (3.17)
Global Aβ SUVR	1.29 (±0.29; 0.99–2.45)
Meta-ROI tau SUVR	1.15 (±0.10; 0.85–1.61)

Note: Data are depicted as the mean (standard deviation; range), except in the case of categorical variables, where the count and percentage are presented.
Abbreviations: Aβ, amyloid-β; APOE, apolipoprotein E; F, female; HDL, high-density lipoprotein; LDL, low-density lipoprotein; MMSE, Mini-Mental State Examination; spEYO, sporadic parental estimated years to symptom onset (age of the person minus age of the parental onset); SUVR, standardized uptake value ratio; WMH, white matter hyperintensity.
[a]MMSE score was available for 187 participants.
[b]Total WMH load was available for 185 participants.
[c]Plasma lipid concentration data (LDL and HDL) were available for 184 participants.

and years of education), genetics (APOE ε4 status), total WMH load, and vascular factors (i.e., cholesterol levels and medical history of hypertension/diabetes). Further information on these measurements is provided in Table 1. Univariate Pearson's correlations between each white matter measurement and individual demographic, genetic, total WMH load and vascular factors are also presented in Supplementary results. All the analyses except for the PLS were performed using R software (version 4.2.1). The PLS analyses were conducted using the pyls Python package (https://github.com/netneurolab/pypyls) with Python 3.8.12 (step 6 in Figure 1 and Supplementary methods).

3 | RESULTS

3.1 | Demographics

Demographic and clinical characteristics of the participants are depicted in Table 1.

3.2 | Aβ, tau, and annual change in memory scores

As hypothesized, we first revealed associations between Aβ/tau burden and changes in immediate memory (Aβ: standardized β [β_{st}] = −0.28, 95% standardized confidence interval [CI_{st}] = [−0.42, −0.14], $R^2 = 0.08$, $p = 1.30 \times 10^{-4}$; tau: $\beta_{st} = -0.34$, 95% CI_{st} = [−0.48, −0.20], $R^2 = 0.12$, $p = 1.00 \times 10^{-5}$) and delayed memory (Aβ: $\beta_{st} = -0.26$, 95% CI_{st} = [−0.40, −0.12], $R^2 = 0.09$, $p = 3.70 \times 10^{-4}$; tau: $\beta_{st} = -0.26$, 95% CI_{st} = [−0.40, −0.12], $R^2 = 0.09$, $p = 3.60 \times 10^{-4}$) (Figure 2).

3.3 | Aβ, tau, and white matter properties

We then found that increased tau pathology was associated with decreased global efficiency in both networks (limbic network: $\beta_{st} = -0.15$, 95% CI_{st} = [−0.29, −0.01], $R^2 = 0.09$, $p = 3.80 \times 10^{-2}$; DMN: $\beta_{st} = -0.18$, 95% CI_{st} = [−0.31, −0.05], $R^2 = 0.25$, $p = 6.21 \times 10^{-3}$) as shown in Figure 3. Additionally, higher tau levels were associated with higher MD_T, RD_T, and FW index within the tracts of the limbic network (MD_T: $\beta_{st} = 0.19$, 95% CI_{st} = [0.05, 0.34], $R^2 = 0.07$, $p = 8.91 \times 10^{-3}$; RD_T: $\beta_{st} = 0.18$, 95% CI_{st} = [0.03, 0.32], $R^2 = 0.03$, $p = 2.01 \times 10^{-2}$; FW index: $\beta_{st} = 0.17$, 95% CI_{st} = [0.02, 0.31], $R^2 = 0.07$, $p = 2.17 \times 10^{-2}$). No associations were observed between any diffusion measures within the tracts of the DMN and tau pathology. Meanwhile, we did not find any significant associations between Aβ pathology and white matter measurements (Figure 3).

3.4 | Global efficiency and cognitive resilience

When adding global efficiency as an interactive term in the models to test the association between AD pathology and change in memory scores, we found that global efficiency in the limbic network moderates the association between tau pathology and both immediate ($\beta_{st} = 0.15$, 95% CI_{st} = [0.01, 0.29], $R^2 = 0.15$, $p = 3.36 \times 10^{-2}$) and delayed ($\beta_{st} = 0.25$, 95% CI_{st} = [0.11, 0.39], $R^2 = 0.17$, $p = 4.50 \times 10^{-4}$) memory decline (Figure 4A,B). Specifically, individuals exhibiting higher global efficiency in the limbic network demonstrated less severe immediate and delayed memory decline in the presence of tau pathology, whereas those with lower global efficiency experienced more pronounced memory decline. We did not find a moderation effect in the relationship between Aβ pathology and longitudinal memory changes (immediate memory change: $\beta_{st} = 0.07$, 95% CI_{st} = [−0.10, 0.24], $R^2 = 0.10$, $p = 4.23 \times 10^{-1}$; delayed memory change: $\beta_{st} = 0.14$, 95% CI_{st} = [−0.02, 0.31], $R^2 = 0.12$, $p = 9.16 \times 10^{-2}$) (Figure S4A,B). Global efficiency of the DMN did not moderate the association between tau pathology and changes in either immediate memory ($\beta_{st} = 0.09$, 95% CI_{st} = [−0.05, 0.22], $R^2 = 0.13$, $p = 2.12 \times 10^{-1}$) or delayed memory ($\beta_{st} = 0.10$, 95% CI_{st} = [−0.04, 0.24], $R^2 = 0.10$, $p = 1.69 \times 10^{-1}$) (Figure 4C,D). Similarly, global efficiency of the DMN showed no moderation effect on the association between Aβ pathology and longitudinal memory changes (immediate memory change: $\beta_{st} = 0.01$, 95% CI_{st} = [−0.13, 0.15], $R^2 = 0.09$, $p = 8.94 \times 10^{-1}$; delayed memory change: $\beta_{st} = 0$, 95% CI_{st} = [−0.14, 0.14], $R^2 = 0.09$, $p = 9.85 \times 10^{-1}$) (Figure S4C,D). We found no mediation effect of global efficiency on the association between AD pathology and memory decline (Tables S7–S10).

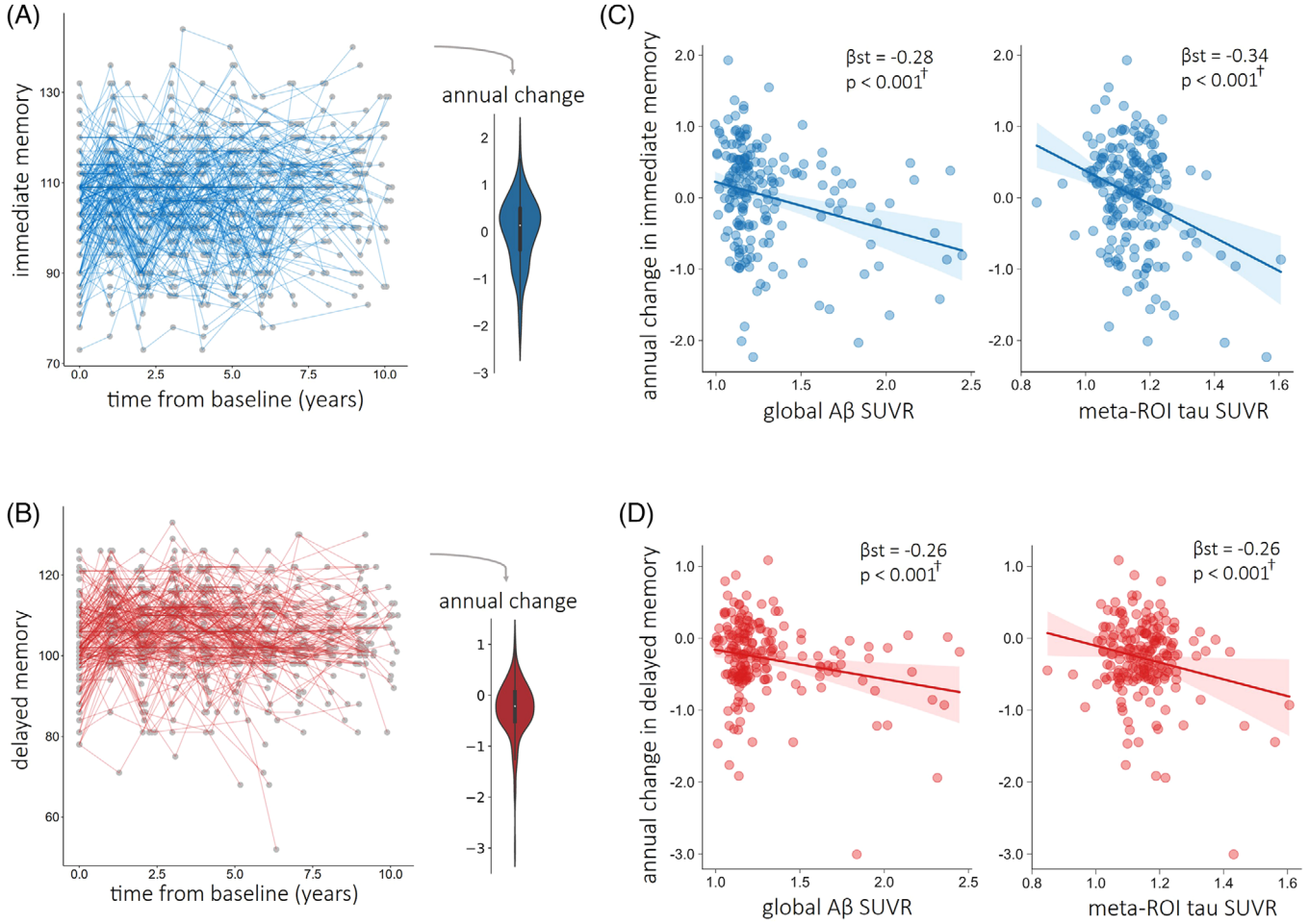

FIGURE 2 Longitudinal memory change and associations with AD pathology. Annual memory changes were calculated based on the longitudinal RBANS data using linear mixed-effects models, and the average of annual changes for immediate memory and delayed memory are shown in (A, B). The associations between Aβ-/tau-pathology are displayed in (C, D). Higher levels of both Aβ and tau pathology were associated with worse immediate and delayed memory decline. Linear models were adjusted for age and sex. Uncorrected two-sided *p*-values are presented; † indicates adjusted *p*-value ≤ 0.05 after FDR correction. β_{st}: standardized estimate β; Aβ, amyloid-β; AD, Alzheimer's disease; FDR, false discovery rate; RBANS, Repeatable Battery for the Assessment of Neuropsychological Status.

3.5 | Micro-structural measurements and cognitive resilience

For the diffusion metrics within the tracts of the limbic network, we found that higher FA_T attenuated the association between tau pathology and delayed memory decline (β_{st} = 0.22, 95% CI_{st} = [0.07, 0.36], R^2 = 0.15, $p = 3.60 \times 10^{-3}$) but not between tau pathology and immediate memory (β_{st} = 0.14, 95% CI_{st} = [−0.00, 0.29], R^2 = 0.14, $p = 5.47 \times 10^{-2}$) (Figure 5A,B). Furthermore, lower MD_T and lower RD_T showed attenuated effects of tau pathology on both immediate (MD_T: $\beta_{st} = -0.14$, 95% $CI_{st} = [-0.25, -0.03]$, $R^2 = 0.15$, $p = 1.42 \times 10^{-2}$; RD_T: $\beta_{st} = -0.16$, 95% $CI_{st} = [-0.29, -0.04]$, $R^2 = 0.15$, $p = 9.60 \times 10^{-3}$) and delayed memory change (MD_T: $\beta_{st} = -0.13$, 95% $CI_{st} = [-0.24, -0.02]$, $R^2 = 0.13$, $p = 2.22 \times 10^{-2}$; RD_T: $\beta_{st} = -0.18$, 95% $CI_{st} = [-0.31, -0.06]$, $R^2 = 0.15$, $p = 3.80 \times 10^{-3}$), while lower FW index within the tracts of the limbic network was associated with less severe immediate memory decline as tau pathology increased ($\beta_{st} = -0.08$, 95% $CI_{st} = [-0.17, -0.00]$, R^2 = 0.14, $p = 4.83 \times 10^{-2}$) (Figure 5A,B). Similar to what was found with global efficiency, none of the FW-corrected diffusion metrics in the limbic network moderated the effect of Aβ pathology on either immediate or delayed memory change (Figure S5A,B). Regarding the DMN tracts, we found that MD_T and FW index moderated the association between tau pathology and immediate memory change (MD_T: $\beta_{st} = -0.12$, 95% $CI_{st} = [-0.24, -0.00]$, R^2 = 0.15, $p = 4.85 \times 10^{-2}$; FW: $\beta_{st} = -0.19$, 95% $CI_{st} = [-0.33, -0.05]$, $R^2 = 0.16$, $p = 7.70 \times 10^{-3}$) while FA_T acted as a moderator between tau pathology and delayed memory change (β_{st} = 0.21, 95% CI_{st} = [0.06, 0.36], R^2 = 0.14, $p = 6.50 \times 10^{-3}$) (Figure 5C,D). Additionally, we found that RD_T within the tracts of the DMN moderated the association between tau pathology and immediate ($\beta_{st} = -0.13$, 95% $CI_{st} = [-0.26, -0.01]$, R^2 = 0.16, $p = 3.66 \times 10^{-2}$) and delayed memory change ($\beta_{st} = -0.13$, 95% $CI_{st} = [-0.26, -0.01]$, R^2 = 0.12, $p = 4.12 \times 10^{-2}$) (Figure 5C,D). Again, we did not find evidence to suggest that white matter micro-structural properties of the DMN moderated the association between Aβ pathology and longitudinal memory changes (Figure 5C,D). Additionally, white matter micro-structural measurements of

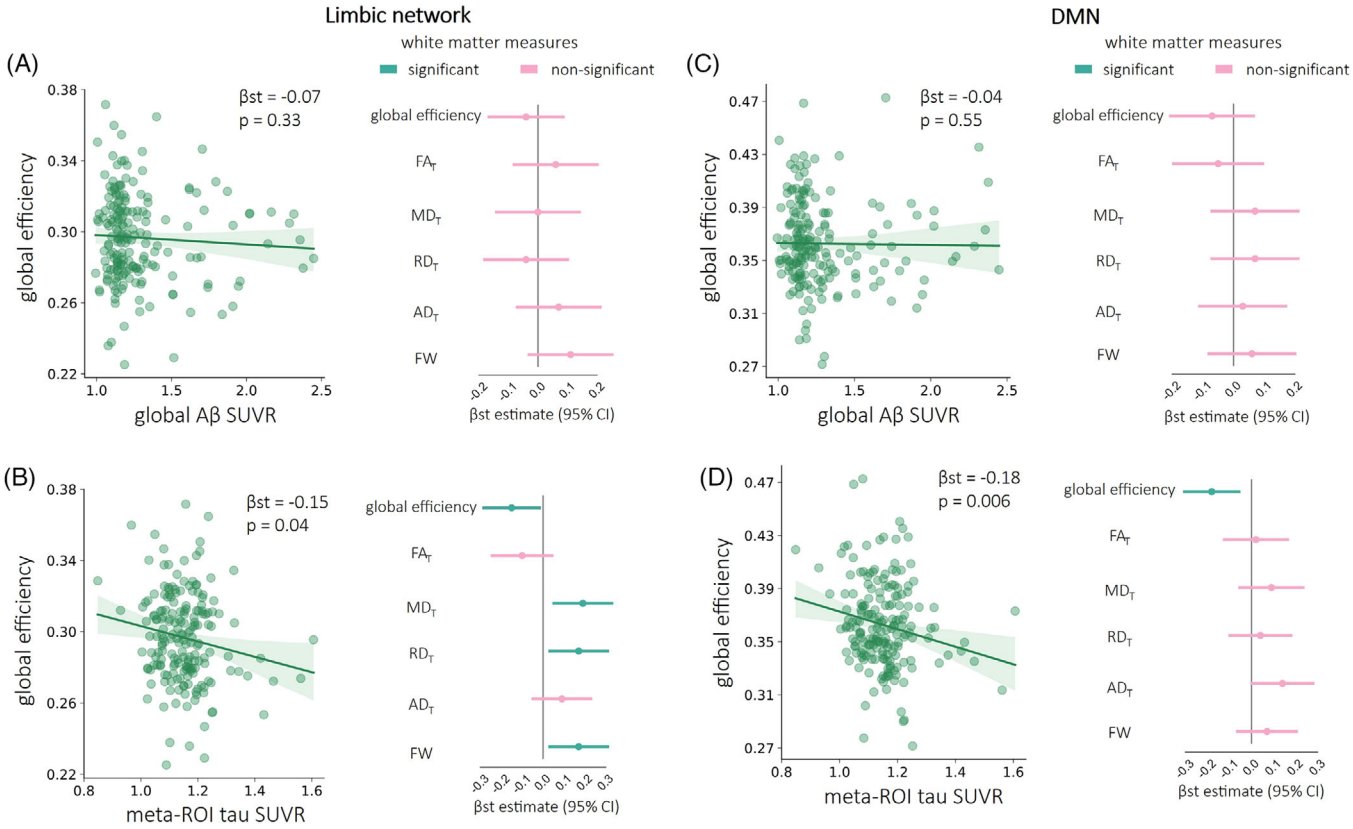

FIGURE 3 Association between Aβ/tau pathology and macro-/micro-structural white matter measurements. The scatter plots show the association between Aβ/tau pathology and global efficiency of the limbic network (A, B) and the DMN (C, D). Linear models were adjusted for age and sex. β_{st} estimates and 95% standardized CIs, obtained from linear regression models incorporating various white matter measures as dependent variables are displayed on the right of each panel. Light green represents significant β_{st} estimates for the association between Aβ/tau pathology and white matter measures, and pink represents non-significant β_{st} estimates. Aβ, amyloid-β; AD_T, free-water corrected axial diffusivity; β_{st}, standardized estimate β; CI, confidence interval; DMN, default mode network; FA_T, free-water corrected fractional anisotropy; FW, free-water index; MD_T, free-water corrected mean diffusivity; RD_T, free-water corrected radial diffusivity.

both networks did not mediate the association between AD pathology and memory changes (Tables S7–S10).

3.6 | Macro-/micro-structural measurements and health/risk factors

For the PLS analysis between white matter characteristics of the limbic network and health/lifestyle factors, one significant latent variable emerged ($p = 1.00 \times 10^{-4}$), explaining 71.69% of the covariance in the data. Figure 6A displays the bootstrap ratios for white matter measurements of the limbic network and loadings of the factors for this latent variable. In this association pattern, we observed that lower education, female sex, greater WMH burden, and a history of hypertension were conjointly associated with reduced global efficiency, decreased FA_T, and increased MD_T, RD_T, and FW index within tracts of the limbic network. Regarding the DMN, there were two significant latent variables explaining 67.81% and 23.23% of the cross-block covariance, respectively ($p = 1.00 \times 10^{-4}$, $p = 9.00 \times 10^{-3}$). The bootstrap ratios and loadings for the first latent variable are shown in Figure 6B. A combination of lower LDL value, older age, greater WMH burden and a history of hypertension were related to lower FA_T, and higher MD_T, RD_T, and FW index within tracts of the DMN, while global efficiency did not contribute to this pattern. The results for the second latent variable are presented in Figure S6. Univariate analyses corroborate the PLS findings, with detailed information available in Figure S7.

4 | DISCUSSION

Resilience to AD pathology refers to the capacity of certain persons/brains to maintain more optimal cognitive performance despite the presence of AD pathology. This phenomenon, while extremely important, is poorly understood. Increasing evidence suggests that protective lifestyle factors may play a role in cognitive resilience.[11-13] Leveraging a longitudinal cohort of cognitively unimpaired older adults at increased risk of AD, we investigated whether macro-/micro-structural white matter properties influence cognitive resilience to AD pathology in vivo. More specifically, we tested whether global efficiency of the limbic network and the DMN, or diffusion metrics within

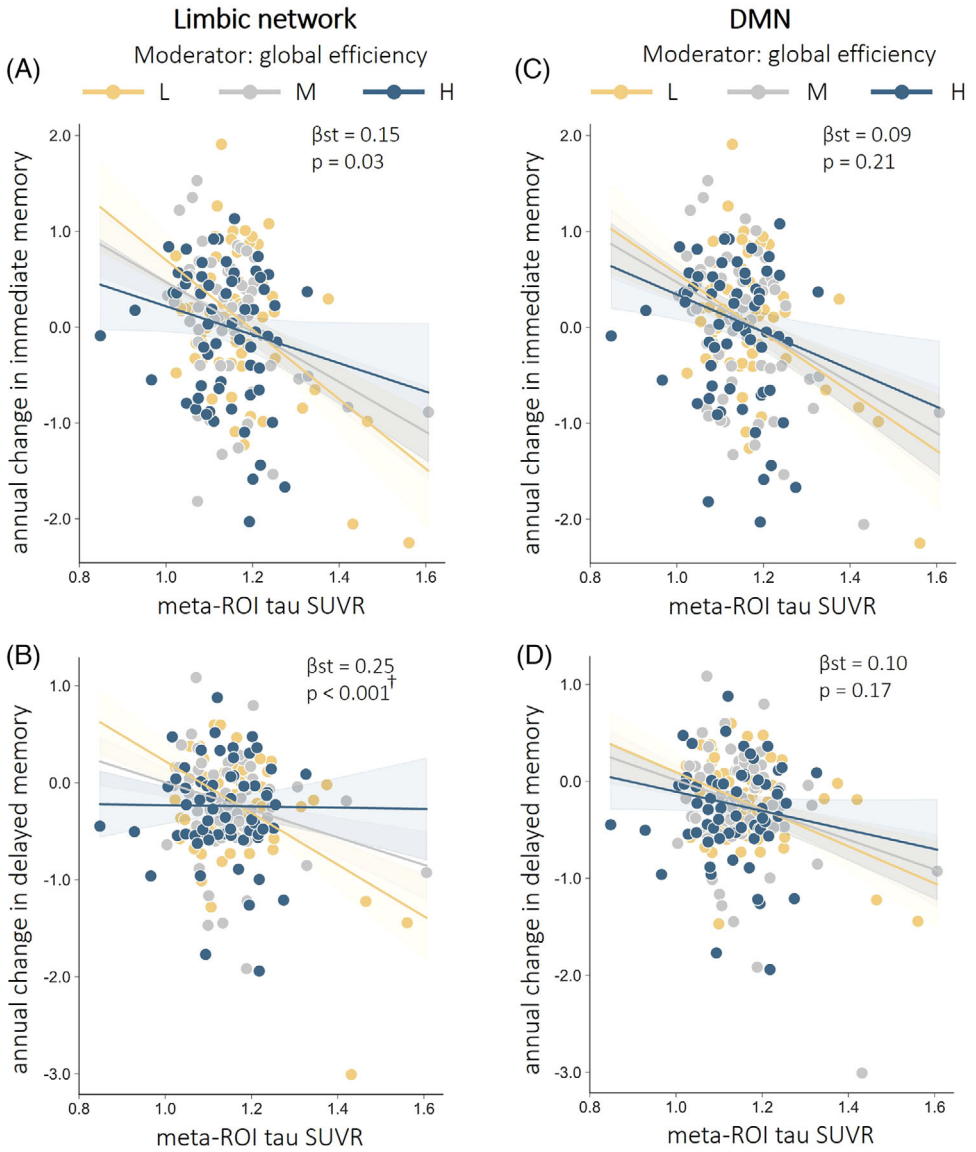

FIGURE 4 Moderation by global efficiency on the association between tau pathology and longitudinal memory change. In the limbic network, higher global efficiency was associated with an attenuated effect of tau burden on both changes in immediate memory (A) and changes in delayed memory (B). The global efficiency of the DMN showed a non-significant moderation effect on the association between tau pathology on both change in immediate memory (C) and change in delayed memory (D). Note that moderation effects were assessed using continuous values of global efficiency, and the data were subsequently divided into terciles for visualization purposes. Specifically, the lowest tercile contains the lower third of the data distribution (L; colored in yellow), the middle tercile spans the middle third (M; colored in light gray), and the upper tercile covers the upper third (H; colored in dark blue). Age, sex, and gray matter volume (divided by total intracranial volume) of regions for the limbic network or the DMN were adjusted for in linear models. Uncorrected two-sided *p*-values are presented; † indicates adjusted *p*-value ≤ 0.05 after FDR correction. β_{st}: standardized estimate β; DMN, default mode network.

the tracts of these two networks, moderate the association between Aβ/tau pathology and longitudinal memory change over ~7.5 years of cognitive follow-up. At the macro-structural level, we found that higher levels of global efficiency of structural networks (especially in the limbic network) were associated with an attenuated effect of tau pathology on delayed memory decline. Then, from a micro-structural perspective, we observed that higher FA_T, lower MD_T, lower RD_T, and lower FW index within the tracts of the limbic network and of the DMN mitigate the effect of tau pathology on longitudinal delayed memory decline. Notably, our study did not uncover any influence of white matter properties on the impact of Aβ pathology on memory change. Given that AD pathology also influenced white matter properties, as a last step, we examined the association between white matter characteristics of both networks and health/risk factors with the aim to identify factors that could influence white matter integrity. We found that lower education, older age, female sex, greater WMH burden, and

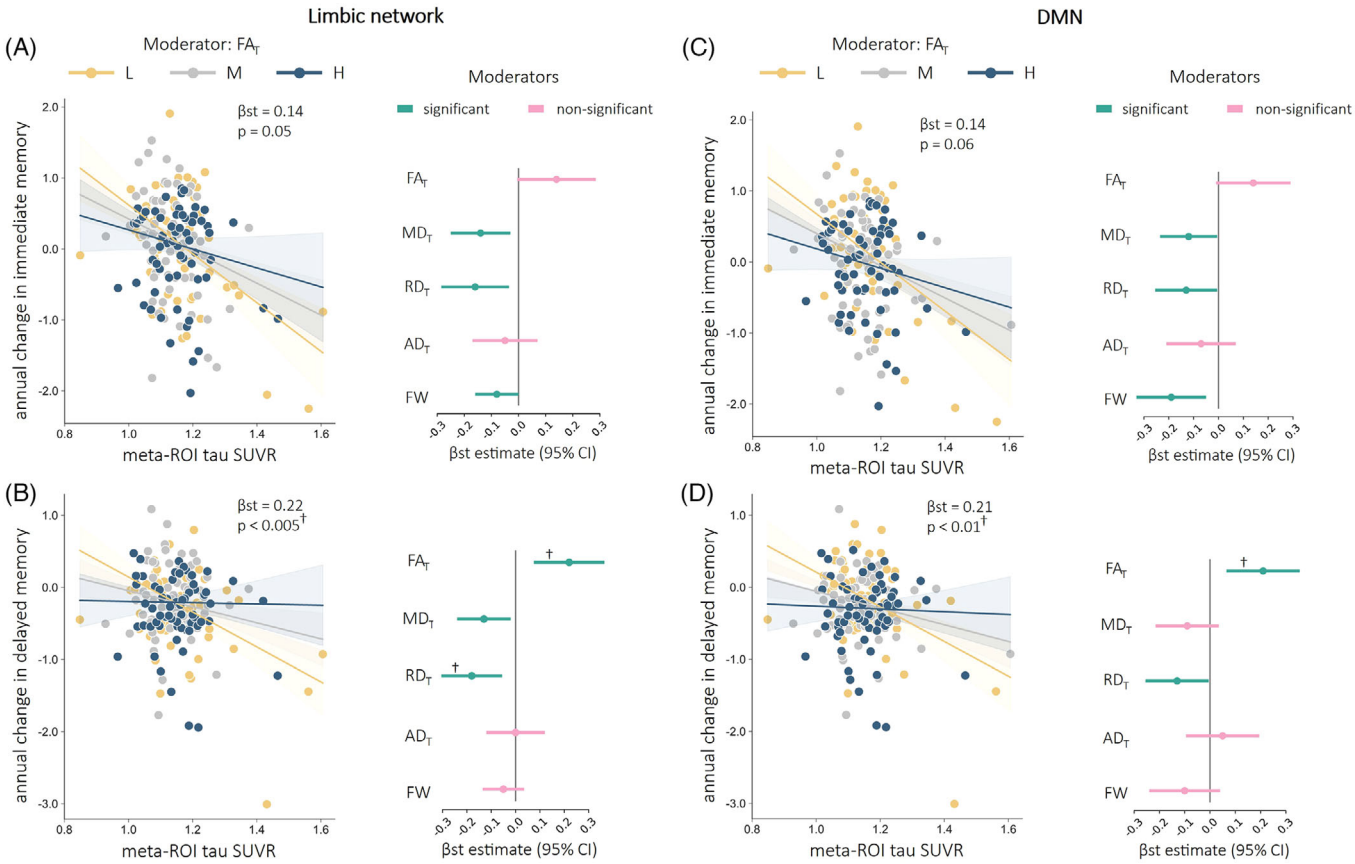

FIGURE 5 Moderation by diffusion metrics on the association between tau pathology and longitudinal memory change. The moderating effects of diffusion metrics within the limbic network (A, B) and DMN (C, D) on the impact of tau pathology on immediate and delayed memory change. The scatter plots in each panel show that FA_T in the tracts acts as a moderator on the association between tau burden and longitudinal memory changes. Note that moderation effects were assessed using continuous values of diffusion metrics (average diffusion metrics in the tracts of the limbic network or the DMN), and the data were subsequently divided into terciles for visualization purposes. Specifically, the lowest tercile contains the lower third of the data distribution (L; colored in yellow), the middle tercile spans the middle third (M; colored in light gray), and the upper tercile covers the upper third (H; colored in dark blue). Age, sex, and gray matter volume (divided by total intracranial volume) of regions for the limbic network or DMN were adjusted for in linear models. Uncorrected two-sided *p*-values are presented; † indicates adjusted *p*-value ≤ 0.05 after FDR correction. β_{st} estimates and 95% standardized CIs, obtained from linear regression models incorporating various diffusion measures as interaction terms, are displayed on the right of each panel. Light green represents significant β_{st} estimates for the moderation effect of diffusion metrics and pink represents non-significant β_{st} estimates. AD_T, free-water corrected axial diffusivity; CI, confidence interval; DMN, default mode network; FA_T, free-water corrected fractional anisotropy; β_{st}, standardized estimate β; FDR, false discovery rate; FW, free-water index; MD_T, free-water corrected mean diffusivity; RD_T, free-water corrected radial diffusivity.

a history of hypertension were associated with worse white matter properties as shown by decreased global efficiency of the limbic network, as well as decreased FA_T, increased MD_T, RD_T, and FW index within tracts of both networks. Taken together, these findings suggest that both macro- and micro-structural white matter properties of the limbic network and the DMN play a role in determining cognitive performance in the face of tau pathology in the preclinical stages of AD and that a healthy vascular lifestyle may promote optimal white matter properties.

While most studies in AD focus on gray matter,[55,56] white matter is hypothesized to be among the earliest brain structures impacted in the course of the disease.[57] By acting as a communication conduit between various gray matter regions, white matter plays a key role in several cognitive processes including immediate and delayed memory, processing speed, executive functions, and global cognition.[58,59] Numerous studies have shown that white matter abnormalities are associated with worse cognitive decline in individuals with mild cognitive impairment (MCI) and AD dementia.[60-65] Decreased global efficiency in structural networks is increasingly recognized as a key component of cognitive deficit severity in MCI and AD patients.[63-65] At the micro-structural level, reductions in FA and elevations in MD are commonly observed as indicators of compromised white matter in addition to being associated with cognitive decline in individuals with MCI and AD.[66,67] Our findings have further highlighted the significance of network performance and underlying micro-structural properties in maintaining optimal memory performance in the preclinical phase of AD. We found that structural global efficiency in the limbic network and the DMN as well as micro-structural white matter characteristics

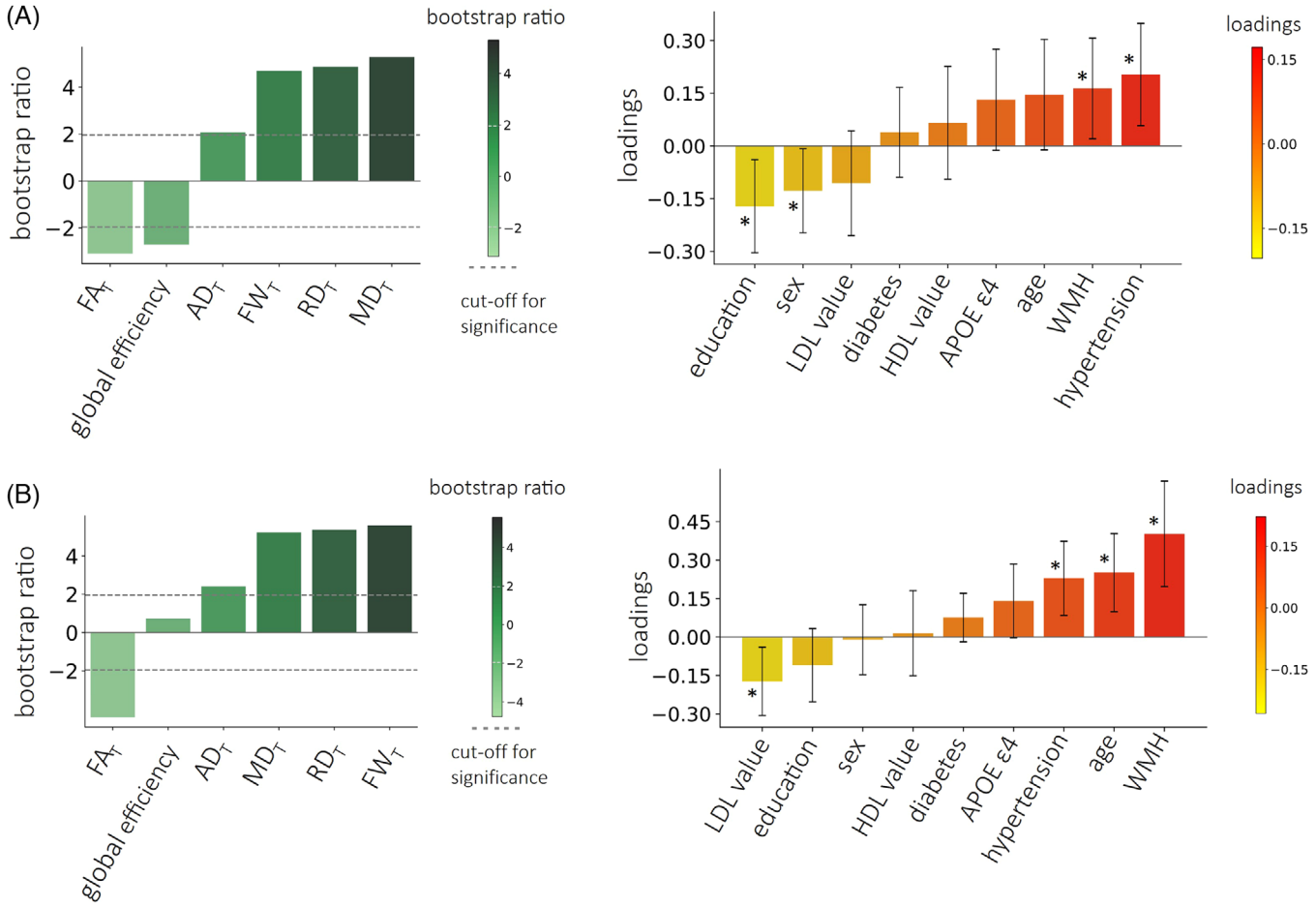

FIGURE 6 Results of the PLS analyses between white matter characteristics and health/risk factors. In each panel, the magnitude of the bootstrap ratios for white matter measurements within the limbic network (A) and DMN (B) are depicted using a gradient green color scale on the left. The significance threshold is indicated by dotted lines; bootstrap ratios of white matter measurements above/below the dotted lines are considered as significant variables contributing to the association pattern. On the right side of each panel, the strengths of the loadings for the health/risk factors are shown in a gradient orange hue, with error bars representing bootstrap-estimated 95% confidence intervals; * indicates significant factors that contributed to the association pattern. AD_T, free-water corrected axial diffusivity; DMN, default mode network; FA_T, free-water corrected fractional anisotropy; FW, free-water index; HDL, high-density lipoprotein; LDL, low-density lipoprotein; MD_T, free-water corrected mean diffusivity; PLS, partial least square; RD_T, free-water corrected radial diffusivity; WMH, white matter hyperintensity.

within the tracts of these networks could help reduce memory decline associated with tau pathology. Importantly, this protective effect was present prior to cognitive impairments, possibly postponing the clinical expression of the disease in individuals with preclinical AD.

Surprisingly, even in the DMN, a network commonly associated with Aβ deposition, we did not identify any evidence indicating that white matter properties modify the association between Aβ pathology and memory decline. While we hypothesized a protective effect of white matter properties on both Aβ and tau-related cognitive decline, tau appears more closely related to neurodegeneration[68] and cognitive decline than Aβ plaques,[69] and it is possible that the protective effect of white matter on memory decline is simply more apparent with tau than Aβ.

Our findings further indicate that education, age, sex, WMH burden, and a history of hypertension were all associated with white matter properties. These results emphasize the potential influence of sociodemographic factors and health history on the structural integrity of the brain's communication pathways. While certain factors, such as inherent aging processes, are beyond our control, we can promote education and manage cardiovascular risk factors through appropriate lifestyle and medical care. These efforts could play a pivotal role in increasing both brain resistance and resilience to AD pathology.[70-72] Although further research is warranted to elucidate the underlying mechanisms driving these associations, our findings underscore the significance of identifying protective factors to support healthy brain aging and potentially mitigate tau-related memory decline in the early phase of AD.

A main limitation of this study is the comparatively small number of participants with high tau burden, although this is expected in cognitively unimpaired individuals.[73,74] To partly counteract this limitation, we used tau as a continuous variable, based on the fact that tau accumulates over years, and it is usually present before people reach the

threshold for positivity. Still, modest associations were detectable, and the results were corroborated across different white matter measures, supporting the plausibility of these associations. Importantly, increased tau was also associated with reduced global efficiency in both networks and to a lesser extent with MD_T, RD_T, and FW index of the limbic network. We therefore cannot neglect that part of our moderation effect were driven by the negative impact of tau pathology on white matter. To address this, we tested whether white matter properties mediate the association between tau and cognition and found no results supporting this pathway. Finally, this study employed a standard atlas for network node definition. Future research may delve into individualized parcellation methods to examine the nuances of finer-scale functional variability across individuals. A main strength of the study is the use of high-quality diffusion MRI data, complemented by the advanced FW-corrected DTI model. Future studies could benefit from exploring other techniques, such as fixel-based measures and neurite orientation dispersion and density imaging.

Overall, our findings indicate that white matter properties influence the association between tau pathology and cognitive performance in cognitively unimpaired adults with a family history of sporadic AD. These results provide support for measures aiming at maintaining white matter health in the context of cognitive change during the progression of AD. Our study contributes valuable insights for future research targeting the prediction of cognitive decline, designing interventions to improve cognitive resilience, and delaying the clinical onset of AD dementia.

ACKNOWLEDGMENTS

This work was supported by fellowship from Chinese Scholarship Council (201906070287; to T.Q.); Healthy Brains, Healthy Lives scholarship from McGill University (to T.Q.); Recruitment Scholarship from Quebec (to T.Q.). The PREVENT-AD (Pre-symptomatic Evaluation of Experimental or Novel Treatments for Alzheimer's Disease) data were funded by a Canadian Institutes of Health Research foundation grant, an Alzheimer's Association grant, a joint Alzheimer's Society Canada and Brain Canada Research grant, a National Institutes of Health grant and a Lemaire foundation donation. The authors thank Jordana Remz, Yara Yakoub, Bery Mohammediyan, Valentin Ourry, Jonathan Gallego Rudolf, Mohammadali Javanray, and Brandon Hall for helpful discussions and feedback for this study. We thank all the participants in the PREVENT-AD.

CONFLICT OF INTEREST STATEMENT

The authors declare no conflicts of interest. Author disclosures are available in the supporting information.

DATA AVAILABILITY STATEMENT

Data used for this study were obtained from the Pre-symptomatic Evaluation of Experimental or Novel Treatments for Alzheimer's Disease (PREVENT-AD) study. Some of these data are openly accessible at https://openpreventad.loris.ca and https://registeredpreventad.loris.ca. Additional data from this study can be made available upon approval by the scientific committee at the Centre for Studies on Prevention of Alzheimer's Disease (StoP-AD) at the Douglas Mental Health University Institute.

CONSENT STATEMENT

All participants provided written informed consent and the Institutional Review Board at McGill University approved all research procedures.

REFERENCES

1. Duyckaerts C, Delatour B, Potier MC. Classification and basic pathology of Alzheimer disease. *Acta Neuropathologica*. 2009;118(1):5-36. doi:10.1007/s00401-009-0532-1
2. Vogel JW, Iturria-Medina Y, Strandberg OT, et al. Spread of pathological tau proteins through communicating neurons in human Alzheimer's disease. *Nat Commun*. 2020;11(1):2612. doi:10.1038/s41467-020-15701-2
3. Pereira JB, Ossenkoppele R, Palmqvist S, et al. Amyloid and tau accumulate across distinct spatial networks and are differentially associated with brain connectivity. *eLife*. 2019;8:e50830. doi:10.7554/eLife.50830
4. Smallwood J, Bernhardt BC, Leech R, Bzdok D, Jefferies E, Margulies DS. The default mode network in cognition: a topographical perspective. *Nat Rev Neurosci*. 2021;22(8):503-513. doi:10.1038/s41583-021-00474-4
5. Teipel S, Grothe MJ, Zhou J, et al. Measuring cortical connectivity in Alzheimer's disease as a brain neural network pathology: toward clinical applications. *JINS*. 2016;22(2):138-163. doi:10.1017/s1355617715000995
6. Andrews-Hanna JR, Smallwood J, Spreng RN. The default network and self-generated thought: component processes, dynamic control, and clinical relevance. *Ann N Y Acad Sci*. 2014;1316(1):29-52. doi:10.1111/nyas.12360
7. Schneider JA, Arvanitakis Z, Leurgans SE, Bennett DA. The neuropathology of probable Alzheimer disease and mild cognitive impairment. *Ann Neurol*. 2009;66(2):200-208. doi:10.1002/ana.21706
8. Nelson PT, Alafuzoff I, Bigio EH, et al. Correlation of Alzheimer disease neuropathologic changes with cognitive status: a review of the literature. *J Neuropathol Exp Neurol*. 2012;71(5):362-381. doi:10.1097/NEN.0b013e31825018f7
9. Zissimopoulos J, Crimmins E, St Clair P. The value of delaying Alzheimer's disease onset. *Forum Health Econ Policy*. 2014;18(1):25-39. doi:10.1515/fhep-2014-0013
10. Ewers M, Luan Y, Frontzkowski L, et al. Segregation of functional networks is associated with cognitive resilience in Alzheimer's disease. *Brain J Neurol*. 2021;144(7):2176-2185. doi:10.1093/brain/awab112
11. Pa J, Aslanyan V, Casaletto KB, et al. Effects of sex, APOE4, and lifestyle activities on cognitive reserve in older adults. *Neurology*. 2022;99(8):e789-e798. doi:10.1212/wnl.0000000000200675
12. Suemoto CK, Bertola L, Grinberg LT, et al. Education, but not occupation, is associated with cognitive impairment: the role of cognitive reserve in a sample from a low-to-middle-income country. *Alzheimers Dement*. 2022;18(11):2079-2087. doi:10.1002/alz.12542
13. Ourry V, Binette AP, St-Onge F, et al. How do modifiable risk factors affect Alzheimer's disease pathology or mitigate its effect on clinical symptom expression? *Biol Psychiatry*. 2023:S0006-3223(23)01562-7. doi:10.1016/j.biopsych.2023.09.003
14. Franzmeier N, Düzel E, Jessen F, et al. Left frontal hub connectivity delays cognitive impairment in autosomal-dominant and sporadic Alzheimer's disease. *Brain*. 2018;141(4):1186-1200. doi:10.1093/brain/awy008
15. DeJong NR, Jansen JFA, van Boxtel MPJ, et al. Cognitive resilience depends on white matter connectivity: the Maastricht Study. *Alzheimers Dementia*. 2023;19(4):1164-1174. doi:10.1002/alz.12758

16. Bullmore E, Sporns O. The economy of brain network organization. *Nat Rev Neurosci*. 2012;13(5):336-349. doi:10.1038/nrn3214
17. Li X, Wang Y, Wang W, et al. Age-related decline in the topological efficiency of the brain structural connectome and cognitive aging. *Cerebral Cortex (New York, NY : 1991)*. 2020;30(8):4651-4661. doi:10.1093/cercor/bhaa066
18. Yu M, Sporns O, Saykin AJ. The human connectome in Alzheimer disease—relationship to biomarkers and genetics. *Nat Rev Neurol*. 2021;17(9):545-563. doi:10.1038/s41582-021-00529-1
19. Zhang HQ, Chau ACM, Shea YF, et al. Disrupted structural white matter network in Alzheimer's disease continuum, vascular dementia, and mixed dementia: a diffusion tensor imaging study. *J Alzheimers Dis*. 2023;94(4):1487-1502. doi:10.3233/jad-230341
20. Fischer FU, Wolf D, Tüscher O, Fellgiebel A. Structural network efficiency predicts resilience to cognitive decline in elderly at risk for Alzheimer's disease. *Front Aging Neurosci*. 2021;13:637002. doi:10.3389/fnagi.2021.637002
21. Pasternak O, Sochen N, Gur Y, Intrator N, Assaf Y. Free water elimination and mapping from diffusion MRI. *Magn Reson Med*. 2009;62(3):717-730. doi:10.1002/mrm.22055
22. Albi A, Pasternak O, Minati L, et al. Free water elimination improves test-retest reproducibility of diffusion tensor imaging indices in the brain: a longitudinal multisite study of healthy elderly subjects. *Hum Brain Mapp*. 2017;38(1):12-26. doi:10.1002/hbm.23350
23. Chang YL, Chao RY, Hsu YC, Chen TF, Tseng WI. White matter network disruption and cognitive correlates underlying impaired memory awareness in mild cognitive impairment. *NeuroImage Clin*. 2021;30:102626. doi:10.1016/j.nicl.2021.102626
24. Zhao H, Cheng J, Liu T, et al. Orientational changes of white matter fibers in Alzheimer's disease and amnestic mild cognitive impairment. *Human brain mapping*. 2021;42(16):5397-5408. doi:10.1002/hbm.25628
25. Breitner JCS, Poirier J, Etienne PE, Leoutsakos JM. Rationale and Structure for a New Center for Studies on Prevention of Alzheimer's Disease (StoP-AD). *The journal of prevention of Alzheimer's disease*. 2016;3(4):236-242. doi:10.14283/jpad.2016.121
26. Tremblay-Mercier J, Madjar C, Das S, et al. Open science datasets from PREVENT-AD, a longitudinal cohort of pre-symptomatic Alzheimer's disease. *NeuroImage Clin*. 2021;31:102733. doi:10.1016/j.nicl.2021.102733
27. Jahn H. Memory loss in Alzheimer's disease. *Dialogues Clin Neurosci*. 2013;15(4):445-454. doi:10.31887/DCNS.2013.15.4/hjahn
28. Desikan RS, Ségonne F, Fischl B, et al. An automated labeling system for subdividing the human cerebral cortex on MRI scans into gyral based regions of interest. *NeuroImage*. 2006;31(3):968-980. doi:10.1016/j.neuroimage.2006.01.021
29. Jagust WJ, Landau SM, Koeppe RA, et al. The Alzheimer's Disease Neuroimaging Initiative 2 PET Core: 2015. *Alzheimers Dement*. 2015;11(7):757-771. doi:10.1016/j.jalz.2015.05.001
30. Baker SL, Maass A, Jagust WJ. Considerations and code for partial volume correcting [(18)F]-AV-1451 tau PET data. *Data Brief*. 2017;15:648-657. doi:10.1016/j.dib.2017.10.024
31. Pichet Binette A, Theaud G, Rheault F, et al. Bundle-specific associations between white matter microstructure and Aβ and tau pathology in preclinical Alzheimer's disease. *eLife*. 2021;10:e62929. doi:10.7554/eLife.62929
32. Jack CR Jr, Wiste HJ, Weigand SD, et al. Defining imaging biomarker cut points for brain aging and Alzheimer's disease. *Alzheimers Dement*. 2017;13(3):205-216. doi:10.1016/j.jalz.2016.08.005
33. Theaud G, Houde JC, Boré A, Rheault F, Morency F, Descoteaux M. TractoFlow: a robust, efficient and reproducible diffusion MRI pipeline leveraging Nextflow & Singularity. *NeuroImage*. 2020;218:116889. doi:10.1016/j.neuroimage.2020.116889
34. Theaud G, Houde J-C, Boré A, Rheault F, Morency F, Descoteaux M. TractoFlow-ABS (Atlas-Based Segmentation). Preprint 2020. https://www.biorxiv.org/content/10.1101/2020.08.03.197384v1
35. Descoteaux M, Angelino E, Fitzgibbons S, Deriche R. Regularized, fast, and robust analytical Q-ball imaging. *Magn Reson Med*. 2007;58(3):497-510. doi:10.1002/mrm.21277
36. Tournier JD, Calamante F, Connelly A. Robust determination of the fibre orientation distribution in diffusion MRI: non-negativity constrained super-resolved spherical deconvolution. *Neuroimage*. 2007;35(4):1459-1472. doi:10.1016/j.neuroimage.2007.02.016
37. Raffelt D, Tournier JD, Rose S, et al. Apparent Fibre Density: a novel measure for the analysis of diffusion-weighted magnetic resonance images. *NeuroImage*. 2012;59(4):3976-3994. doi:10.1016/j.neuroimage.2011.10.045
38. Dell'Acqua F, Simmons A, Williams SC, Catani M. Can spherical deconvolution provide more information than fiber orientations? Hindrance modulated orientational anisotropy, a true-tract specific index to characterize white matter diffusion. *Human brain mapping*. 2013;34(10):2464-2483. doi:10.1002/hbm.22080
39. Rheault FHJ-C, Sidhu J, Obaid S, Guberman G, Daducci A, Descoteaux M. Connectoflow: A cutting-edge Nextflow pipeline for structural connectomics. presented at: International Society for Magnetic Resonance in Medicine (ISMRM); 2021; https://archive.ismrm.org/2021/4301.html
40. Roy M, Rheault F, Croteau E, et al. Fascicle- and Glucose-specific deterioration in white matter energy supply in Alzheimer's Disease. *Journal of Alzheimer's disease : JAD*. 2020;76(3):863-881. doi:10.3233/jad-200213
41. Descoteaux M, Deriche R, Knösche TR, Anwander A. Deterministic and probabilistic tractography based on complex fibre orientation distributions. *IEEE Trans Med Imaging*. 2009;28(2):269-286. doi:10.1109/tmi.2008.2004424
42. Dadar M, Collins DL. BISON: brain tissue segmentation pipeline using T(1) -weighted magnetic resonance images and a random forest classifier. *Magn Reson Med*. 2021;85(4):1881-1894. doi:10.1002/mrm.28547
43. Dadar M, Maranzano J, Misquitta K, et al. Performance comparison of 10 different classification techniques in segmenting white matter hyperintensities in aging. *NeuroImage*. 2017;157:233-249. doi:10.1016/j.neuroimage.2017.06.009
44. Daducci A, Dal Palù A, Lemkaddem A, Thiran JP. COMMIT: convex optimization modeling for microstructure informed tractography. *IEEE Trans Med Imaging*. 2015;34(1):246-257. doi:10.1109/tmi.2014.2352414
45. Schiavi S, Ocampo-Pineda M, Barakovic M, et al. A new method for accurate in vivo mapping of human brain connections using microstructural and anatomical information. *Sci Adv*. 2020;6(31):eaba8245. doi:10.1126/sciadv.aba8245
46. Yeh CH, Jones DK, Liang X, Descoteaux M, Connelly A. Mapping structural connectivity using diffusion MRI: challenges and opportunities. *JMRI*. 2021;53(6):1666-1682. doi:10.1002/jmri.27188
47. Schaefer A, Kong R, Gordon EM, et al. Local-global parcellation of the human cerebral cortex from intrinsic functional connectivity MRI. *Cerebral Cortex (New York, NY : 1991)*. 2018;28(9):3095-3114. doi:10.1093/cercor/bhx179
48. Hansen JY, Shafiei G, Markello RD, et al. Mapping neurotransmitter systems to the structural and functional organization of the human neocortex. *Nat Neurosci*. 2022;25(11):1569-1581. doi:10.1038/s41593-022-01186-3
49. Latora V, Marchiori M. Efficient behavior of small-world networks. *Phys Rev Lett*. 2001;87(19):198701. doi:10.1103/PhysRevLett.87.198701
50. Kurtzer GM, Sochat V, Bauer MW. Singularity: scientific containers for mobility of compute. *PLoS ONE*. 2017;12(5):e0177459. doi:10.1371/journal.pone.0177459

51. Di Tommaso P, Chatzou M, Floden EW, Barja PP, Palumbo E, Notredame C. Nextflow enables reproducible computational workflows. *Nat Biotechnol*. 2017;35(4):316-319. doi:10.1038/nbt.3820
52. Daducci A, Canales-Rodríguez EJ, Zhang H, Dyrby TB, Alexander DC, Thiran JP. Accelerated Microstructure Imaging via Convex Optimization (AMICO) from diffusion MRI data. *NeuroImage*. 2015;105:32-44. doi:10.1016/j.neuroimage.2014.10.026
53. Bocancea DI, Svenningsson AL, van Loenhoud AC, et al. Determinants of cognitive and brain resilience to tau pathology: a longitudinal analysis. *Brain*. 2023;146(9):3719-3734. doi:10.1093/brain/awad100
54. Staekenborg SS, Kelly N, Schuur J, et al. Education as proxy for cognitive reserve in a large elderly memory clinic: 'Window of benefit'. *J Alzheimers Dis*. 2020;76(2):671-679. doi:10.3233/jad-191332
55. Frye BM, Craft S, Register TC, et al. Early Alzheimer's disease-like reductions in gray matter and cognitive function with aging in nonhuman primates. *Alzheimers Dement (N Y)*. 2022;8(1):e12284. doi:10.1002/trc2.12284
56. Dicks E, Vermunt L, van der Flier WM, et al. Modeling grey matter atrophy as a function of time, aging or cognitive decline show different anatomical patterns in Alzheimer's disease. *Neuroimage Clin*. 2019;22:101786. doi:10.1016/j.nicl.2019.101786
57. Araque Caballero M, Suárez-Calvet M, Duering M, et al. White matter diffusion alterations precede symptom onset in autosomal dominant Alzheimer's disease. *Brain*. 2018;141(10):3065-3080. doi:10.1093/brain/awy229
58. Filley CM, Fields RD. White matter and cognition: making the connection. *J Neurophysiol*. 2016;116(5):2093-2104. doi:10.1152/jn.00221.2016
59. Fields RD. White matter in learning, cognition and psychiatric disorders. *Trends Neurosci*. 2008;31(7):361-370. doi:10.1016/j.tins.2008.04.001
60. Radanovic M, Pereira FR, Stella F, et al. White matter abnormalities associated with Alzheimer's disease and mild cognitive impairment: a critical review of MRI studies. *Expert Rev Neurother*. 2013;13(5):483-493. doi:10.1586/ern.13.45
61. Lindemer ER, Greve DN, Fischl B, Salat DH, Gomez-Isla T. White matter abnormalities and cognition in patients with conflicting diagnoses and CSF profiles. *Neurology*. 2018;90(17):e1461-e1469. doi:10.1212/wnl.0000000000005353
62. Garnier-Crussard A, Bougacha S, Wirth M, et al. White matter hyperintensity topography in Alzheimer's disease and links to cognition. *Alzheimers Dement*. 2022;18(3):422-433. doi:10.1002/alz.12410
63. Ajilore O, Lamar M, Kumar A. Association of brain network efficiency with aging, depression, and cognition. *Am J Geriatr Psychiatry*. 2014;22(2):102-110. doi:10.1016/j.jagp.2013.10.004
64. Fathian A, Jamali Y, Raoufy MR. The trend of disruption in the functional brain network topology of Alzheimer's disease. *Sci Rep*. 2022;12(1):14998. doi:10.1038/s41598-022-18987-y
65. Berlot R, Metzler-Baddeley C, Ikram MA, Jones DK, O'Sullivan MJ. Global efficiency of structural networks mediates cognitive control in mild cognitive impairment. *Front Aging Neurosci*. 2016;8:292. doi:10.3389/fnagi.2016.00292
66. Sexton CE, Kalu UG, Filippini N, Mackay CE, Ebmeier KP. A meta-analysis of diffusion tensor imaging in mild cognitive impairment and Alzheimer's disease. *Neurobiol Aging*. 2011;32(12):2322.e5-2322.e18. doi:10.1016/j.neurobiolaging.2010.05.019
67. Power MC, Su D, Wu A, et al. Association of white matter microstructural integrity with cognition and dementia. *Neurobiol Aging*. 2019;83:63-72. doi:10.1016/j.neurobiolaging.2019.08.021
68. Jack CR Jr, Bennett DA, Blennow K, et al. NIA-AA Research Framework: toward a biological definition of Alzheimer's disease. *Alzheimers Dement*. 2018;14(4):535-562. doi:10.1016/j.jalz.2018.02.018
69. Hanseeuw BJ, Betensky RA, Jacobs HIL, et al. Association of amyloid and tau with cognition in preclinical Alzheimer disease: a longitudinal study. *JAMA Neurol*. 2019;76(8):915-924. doi:10.1001/jamaneurol.2019.1424
70. Power MC, Tingle JV, Reid RI, et al. Midlife and late-life vascular risk factors and white matter microstructural integrity: the atherosclerosis risk in communities neurocognitive study. *J Am Heart Assoc*. 2017;6(5):e005608. doi:10.1161/jaha.117.005608
71. Wassenaar TM, Yaffe K, van der Werf YD, Sexton CE. Associations between modifiable risk factors and white matter of the aging brain: insights from diffusion tensor imaging studies. *Neurobiol Aging*. 2019;80:56-70. doi:10.1016/j.neurobiolaging.2019.04.006
72. Arenaza-Urquijo EM, Vemuri P. Resistance vs resilience to Alzheimer disease: clarifying terminology for preclinical studies. *Neurology*. 2018;90(15):695-703. doi:10.1212/wnl.0000000000005303
73. Ossenkoppele R, Pichet Binette A, Groot C, et al. Amyloid and tau PET-positive cognitively unimpaired individuals are at high risk for future cognitive decline. *Nat Med*. 2022;28(11):2381-2387. doi:10.1038/s41591-022-02049-x
74. Strikwerda-Brown C, Hobbs DA, Gonneaud J, et al. Association of elevated amyloid and tau positron emission tomography signal with near-term development of Alzheimer disease symptoms in older adults without cognitive impairment. *JAMA Neurol*. 2022;79(10):975-985. doi:10.1001/jamaneurol.2022.2379

SUPPORTING INFORMATION

Additional supporting information can be found online in the Supporting Information section at the end of this article.

How to cite this article: Qiu T, Liu Z-Q, Rheault F, et al. Structural white matter properties and cognitive resilience to tau pathology. *Alzheimer's Dement*. 2024;1-14. https://doi.org/10.1002/alz.13776

APPENDIX

Collaborators for the PREVENT-AD study is available at this website (https://preventad.loris.ca/acknowledgements/acknowledgements.php?date=2023-03-23).